Dynamic Fractures in PMMA

Suphunnika Manmek & Lerkiat Vongsarnpigoon
Department of Mechanical Engineering, Faculty of Engineering,
Mahanakorn University of Technology, Bangkok, Bangkok 10530
Phone 66(2)988-3655 ext. 244, Fax.66(2)988-3655 ext. 241, E-Mail: suphunni@mut.ac.th

Alojz Ivankovic & Stuart Hillmansen
Department of Mechanical Engineering, Faculty of Engineering,
Imperial College of Science, Technology and Medicine, London, UK

Abstract

This research is aimed to study the rapid crack propagation in polymethylmethacrylate (PMMA) using electrical resistance method for measuring the crack velocity. The crack velocity tests were performed through single-edge-notched-tensile specimen (SENT) with gold strips on four different deep of the notch.

The crack velocity that found to be increased as the depth of the notch decreased, were approximately 650, 500, 400 and 250 ms^{-1} respectively. The crack behaviour was found to be increased sharply as the crack started to initiate but when the crack lengths had grown to a certain distance, the cracks started to decelerate and then oscillated around a constant speed until the specimen fractured completely. Here, the fracture surface was observed using a scanning electrical microscope (SEM). As the results, the mirror-misty-hackle pattern was found on the shallower depth of the notch as well as the higher of the number of the damage on the specimen. Furthermore both virgin material and fracture surface were observed and found that there is no inclusions for the evidence of the nucleation of the parabolic marking.

1. Introduction

Commercially available PMMA is widely used in industry because it is cheap and easily available. However, it is also prone to brittle fracture, which often involves rapid crack propagation (RCP). An understanding of the phenomenon of RCP is important so that it may be possible to predict and prevent unexpected failures during the service lives of polymers, which may lead to the incurrence of high repair costs and possible loss of lives.

One of the characteristics of RCP is the parabolic markings that appear on the fracture surface. Different hypotheses have been brought up regarding the mechanisms of the markings. Smekal [1] suggested that secondary crack fronts are responsible for the creation of the hyperbolic and parabolic markings while Ravi-chandar & Knauss [2] proposed that crack branching was due to voids in the material. Cavities or foreign particles were also observed by Irwin & Kies [3], Leeuwerik [4] and Matsushinge et al. [5].

On the other hand, Cotterell [6] concluded that the density of the parabolic markings should be proportional to the fracture toughness. Doyle [7] found that for PMMA with a high molecular weight, the separation of a thin craze layer ahead of and coplanar with the propagating crack tip occurs at low crack velocities. The dependence of the fracture surface on molecular weight was also suggested by Sanford and Irvin [8], who found that the hyperbolae became smaller and more concentrated as the molecular weight increased.

Another source for understanding RCP has been through the measurement of crack speed. Although the theory suggests that crack speeds should reach the limiting Rayleigh wave speed, C_R, of 925m/s, experimental evidence show that this speed is never reached. Yoffe [9] showed that a crack moving along a straight line would branch off at an angle beyond a critical speed which is approximately 620 m/s while Ravi-Chandar & Knauss [10,11] obtained a crack speed of approximately 487 m/s.

Fineberg et al. [12,13] suggested that a critical crack velocity exists, at which the velocity begins to oscillate while the mean acceleration drops sharply. The changes in the velocity corresponds with the mirror-misty-hackle pattern which appears on the fracture surface. The critical velocity was found to be approximately 330±30 m/s. In a later work, Fineberg et al. [14] associated the critical velocity with the microbranching of cracks. They argued that when the crack velocity exceeded 340 m/s, all of the increase in the fracture energy was due to the increase in the fracture area caused by the microbranch formation.

The present work aims to clarify these previous observations by measuring the crack speed of single-notch-edged-tensile (SENT) specimens and analysing the associated fracture surfaces under the scanning electron and optical microscopes. The electrical resistance method [12,14,15,16] is employed to measure the crack velocity, but using gold as the conductive layer instead of using aluminium [12,14] or graphite [15,16] in previous studies.

2. Experimental setup and procedure

The SENT specimens were 80mm long, 20mm wide and approximately 8mm thick with notch depths of 0.1, 0.5, 1 and 2mm. On one side of the specimens, two gold strips were coated for the fracture and calibration purposes using a sputter coater machine. A conductive silver strip was also painted to connect the gold strips via terminals at

either end of the specimens to the velocity measurement circuit. The circuit was soldered and placed in an aluminum cast box.

The tests were performed on a Universal testing machine at a constant crosshead speed of 2mm/min. The specimens were gripped such that the lower support was allowed to rotate freely in the z axis to provide only the opening mode I fracture loading and to avoid twisting and bending of the specimens. After the specimens had fractured, the calibration gold strip was stationary scratched in a uniform lengths to calibrate the voltage output as a function of crack length. The fracture surface and the area beneath the fracture surface, which had been cut and ground into sections, was observed using the optical microscope and the SEM.

3. Data analysis

Similar voltage-time traces were obtained for the eight specimens, where two are shown in Figure 1. Three stages of the crack propagation can be identified. The time period from minus 120 to minus 40μs (the 'negative' time indicates the position of the pre-trigger of the oscilloscope of 80%) corresponded to the beginning of the test, when the specimen was still being loaded up. The next 40μs corresponded to crack propagation while the plateau in the last 20μs was when the test had completed.

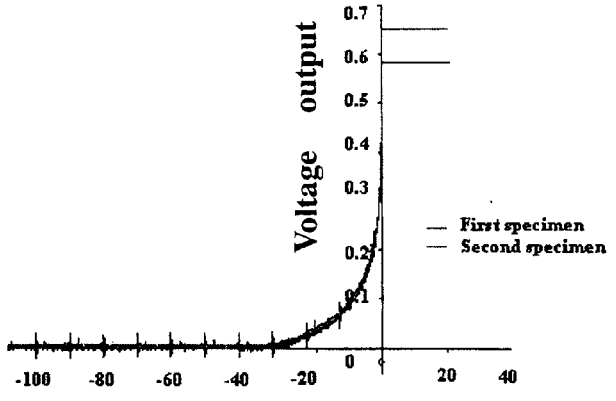

Figure 1 Raw output signal for two 0.1 mm deep specimens.

Since there was considerable noise in the voltage output, the data was smoothed using the FAMOS programme. The smoothing was done by averaging points within a period of time. An estimation of the suitable time period was achieved by dividing the average wavelength of the ripple markings by the average crack speed.

The calibration data was fitted with an exponential function and was then used in conjunction with the voltage-time data to obtain the crack speed data through $\frac{da}{dt} = \frac{da}{dV}\frac{dV}{dt}$ where t is time in seconds, and V is the voltage in volts and a is the corresponding crack length in millimeters. One of the conversion results is presented in Figure 2.

Calibration test

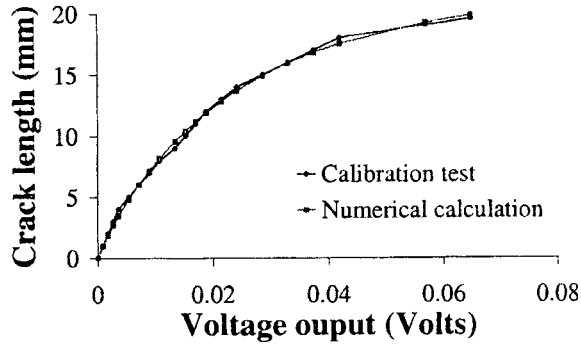

Smoothed data

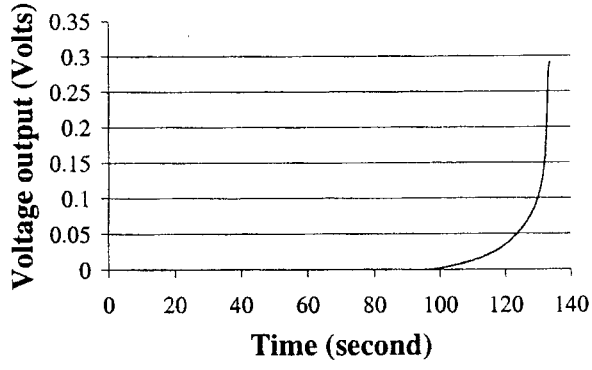

Converted crack length data

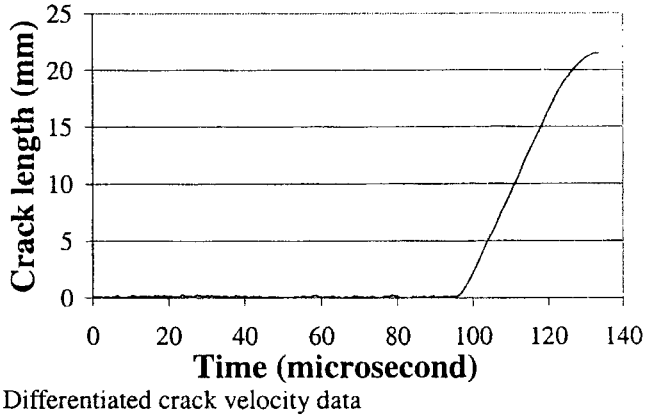

Differentiated crack velocity data

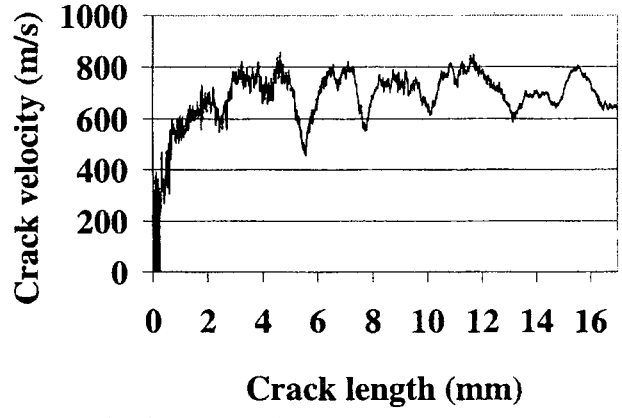

Figure 2 Conversion results for 0.1mm

4. Results

A comparison of the crack speeds for specimens with different notches is shown in Figure 3. The same trend in the variation of crack speed with crack length can be seen for all the specimens. The critical crack speeds for different notch depths were different from each other. They were approximately 650, 500, 400 and 250m/s for the 0.1, 0.5, 1 and 2mm notched respectively. It is therefore not surprising that the specimen with 0.1mm notch gave the shortest fracture time of approximately 25μs. The fracture time were 38, 42 and 60μs for the 0.5, 1 and 2mm notches respectively. Good reproducibility was exhibited for all the specimens as is shown for the 0.5mm specimens in Figure 4.

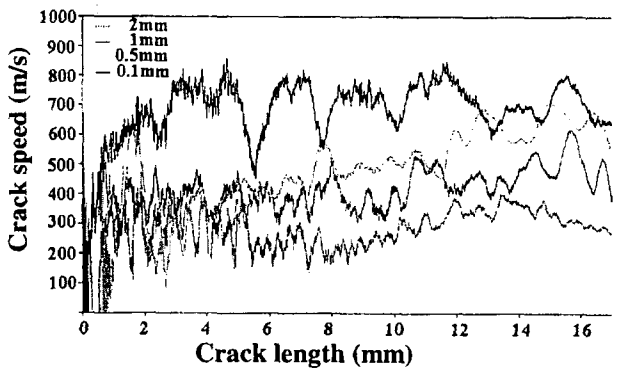

Figure 3 Comparison of crack speed for specimens with different notch depths.

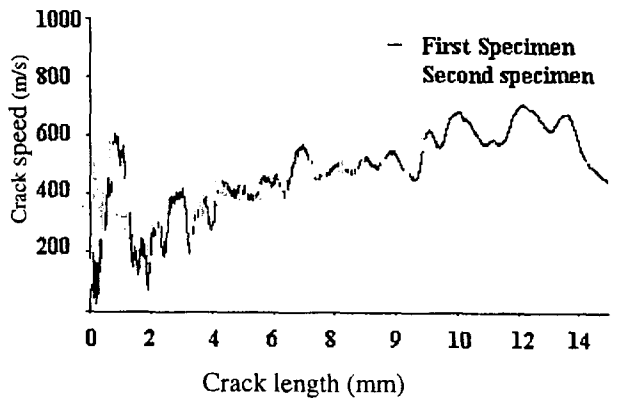

Figure 4 Test results for specimens with notches of 0.5mm

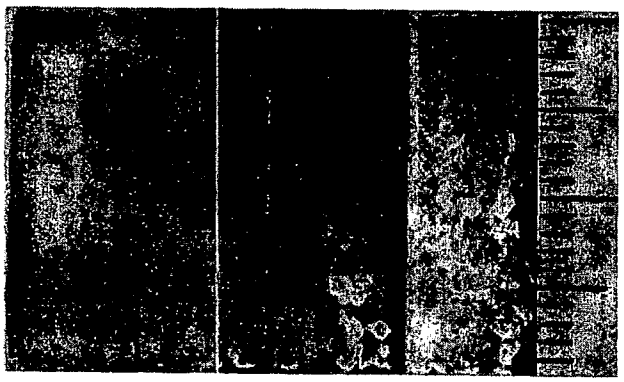

Figure 5 Fracture surfaces for specimens with 2, 1, 0.5 and 0.1 mm notched depth.

Figures 6 and 7 show some images obtained for the fracture surfaces. The 2mm deep specimen gave a mirror-like fracture surface, which corresponded to the constant crack speed. The image beneath the fracture surface was featureless, as shown Figure 5.

Table 1 shows summary of the relationship between the appearance of the fracture surface and number damage marks beneath the surface for different depth of the notch. The 1 mm deep specimen gave an intermediate appearance whereas 0.5mm gave a mirror-misty-hackle which was not very rough surface. Finally, the 0.1mm deep specimen gave a mirror-misty-hackle which was very rough surface was. This specimen cut into four sections for the SEM observations and the results for each section are shown in Figures 6, 9 and 10.

Moreover, the images show no hole at the center of the marking, although there were many holes present all over the fracture surface (Figure 7). Only one foreign particle and a particle were found beneath the fracture surface (see Figure 8). Otherwise no evidence of inhomogeneities or foreign particles were found as well as in virgin materials.

5. Discussion

The crack speed results and the SEM observations appear to correlate well with each other during the initial crack acceleration when the fracture surface exhibited a mirror-like appearance. However, the correlation for the region where the crack speed was oscillating was very difficult to perform since reliable measurements of the oscillation was affected by the noise that was present in the signal. There was a possibility of over or under smoothing the data, which would yield a different trend from the actual data. This procedure is very important and a more thorough study is required in order to obtain more accurate results.

The mirror-misty-hackle pattern was found on the fracture surfaces for specimens with shallow notches (0.5 and 0.1mm deep) while mirror like and intermediate features were found for deeper notches (1 and 2mm). The effect of notch depths on the fracture surface has been noted by other researchers such as Fineberg et al. [12-14]. The amount of damage marks beneath the rough surface was higher than the smooth or intermediate surfaces. This damage is formed by attempted and successful crack branches originated from the main fracture, and other cracks propagating alongside the main fracture. The energy required to create the damage is not taken into account by conventional fracture approaches and this is the main source of inconsistency in correlating measured fracture energies and fracture surface roughness. The SEM examinations revealed that apart from the holes in the vicinity of the parabolic markings, no foreign particles or holes were found elsewhere on the fracture specimen or in the virgin material.

One interesting result which is not shown here was that when a different PMMA sheet was used, a different set of data was obtained. This might be due to the difference in the molecular weight of the test materials even though a regular commercially available cast

PMMA normally has a molecular weight of 1 to 2 million g/mol. This is in support of the observations by Sanford & Irvin [8] and suggests that the initiation of the parabolic markings might be not caused by the inhomogenieties of the material but on the other hand, the molecular chain level might considered to be the reason.

6. Conclusion

The crack speed measurements show that the speeds reach nearly constant mean velocities that were less than the Rayleigh wave speed. The velocity and surface roughness was found to be dependent on the depth of notch. The mirror-misty-hackle pattern was found in a smaller initial deep, which required higher applied loads. Therefore the increasing of the damages were correlates well with the increase in available energy. Examination of the virgin material and fracture surfaces showed no consistent evidence of pre-existing flaws, dust particles or other impurities that would provide nucleation sites for the micro-cracks.

References

[1] Smekal, Glastechnische Berichte, Vol. 23, 1950.

[2] Ravi-Chandar K., Knauss W. G., An experimental investigation into dynamic fracture - III Steady state crack propagation and crack branching,. International Journal of Fracture, Vol. 26, 1984, p.141-154.

[3] Irwin G. R., Kies J. A., Sullivam A. M., Interpretation of fracture markings, Journal of Applied Physics, Vol.21, 1950.

[4] Leeuwerik J., Kinetic features of the brittle fracture phenomenon, Rheologica Acta, Vol. 2, 1962, p.10-16.

[5] Matsushinge K., Sakurada Y., Takahashi K., X-ray microanalysis and acoustic emission studies on the formation mechanism of secondary crack in PMMA, Journal of Materials Science, Vol.19, 1984.

[6] Cotterell B., Fracture propagation in organic glasses, International Journal of Fracture Mechanics, Vol.4, 1968.

[7] Doyle M. J., A mechanism for crack branching in polymethylmethacrylate and the origin of the bands on the surfaces of fracture, Journal of Materials Science, Vol.18, 1958.

[8] Sanford B. N., Wolock I., Fracture phenomena and molecular weight in Polymethylmethacrylate, Journal of Applied Physics, Vol.29, No.1, 1958.

[9] Yoffe E. H., Philos. Mag., Vol.42, 1951.

[10]Ravi-Chandar K., Knauss W. G., An experimental investigation into dynamic fracture - I Crack initiation and crack arrest, International Journal of Fracture, Vol. 25, 1984, p.247-262.

[11]Ravi-Chandar K., Knauss W. G., An experimental investigation into dynamic fracture - II Micro-structural aspects, International Journal of Fracture, Vol.26, 1984, p.65-80.

[12]Ivankovic A., and J. G. Williams, A local modulus analysis of rapid crack propagation in polymers. International Journal of Fracture. Vol. 64, 1993, p.251-268.

[13]Fineberg J., Gross S.P., Maroler M., Swinney H. L. Instability in Dynamic Fracture, Physical Review Letters, The American Physical Society, Vol..67, 1991.

[14]Fineberg J., Gross S.P., Marder M., Swinney H.L., Instability in the propagation of fast cracks, Physical Preview B, The American Physical Society, Vol. 45, 1992.

[15]Sharon E., Fineberg J., Micro-branching instability and the dynamic fracture of brittle materials, Physical Review B, The American Physical Society, 1996.

Table 1 Summary of the SEM observation results

Distance(mm)	The depth of the notch							
	2mm		1mm		0.5mm		0.1mm	
	Appearance as a pattern	Number of Damage marks	Appearance as a pattern	Number of Damage marks	Appearance as a pattern	Number of Damage marks	Appearance as a pattern	Number of Damage marks
2	Mirror							7
8	Mirror	None	parabolic	None	parabolic	1	parabolic	20
12					parabolic	28	Hackle	6
16					Hackle	1	Hackle	27

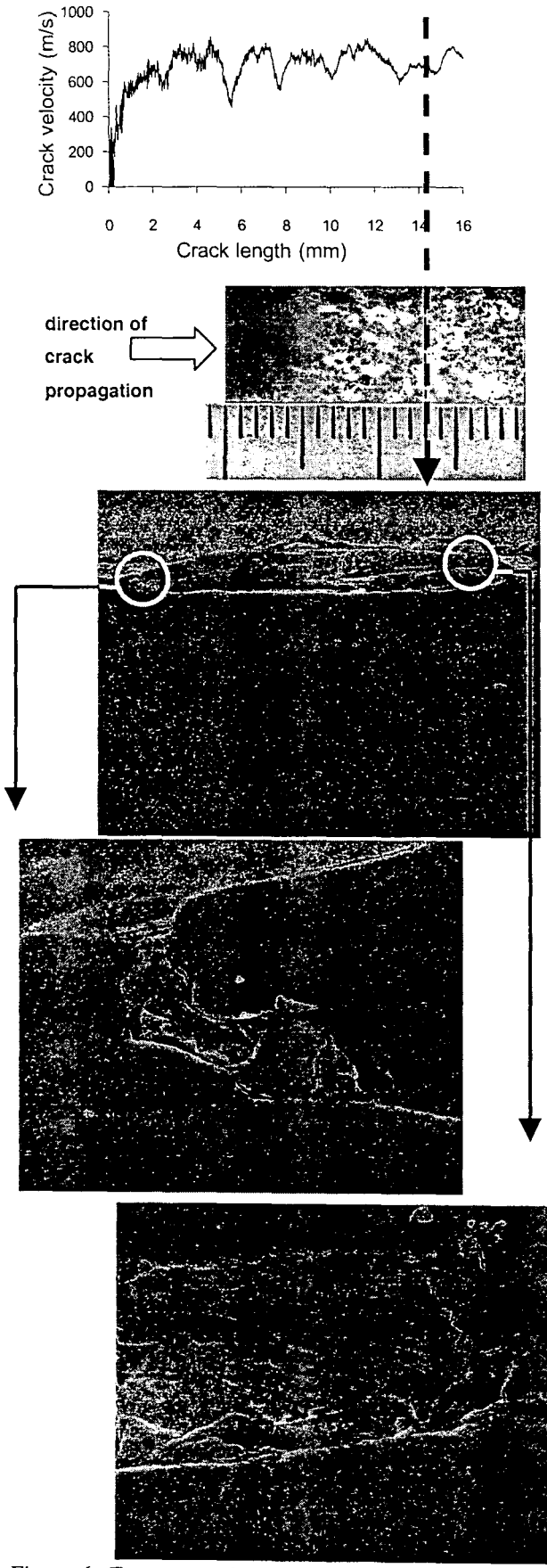

Figure 6 Fracture surface appearance for 0.1mm notch deep specimen at crack length of 13mm using10kV: Top 3.353mm 200×; Bottom left 2000×; Bottom right 2000×

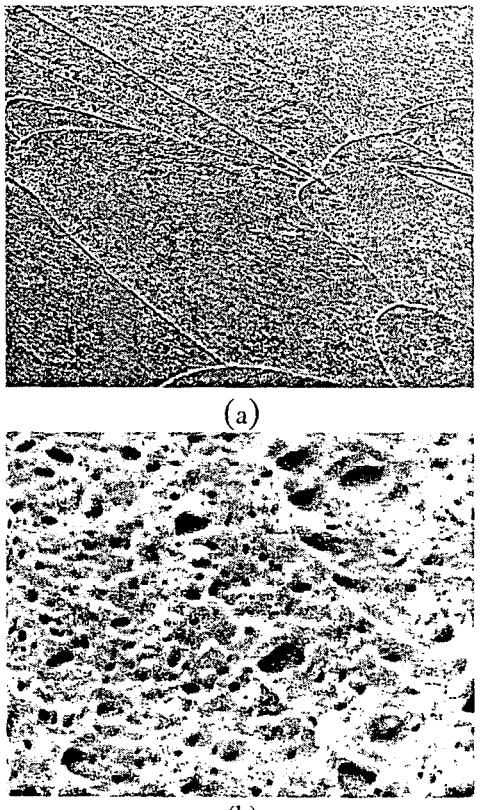

(a)

(b)

Figure 7 (a) Overview image of parabolic markings taken at a magnification of 350x b) Magnified image of Figure 8a at 15000x

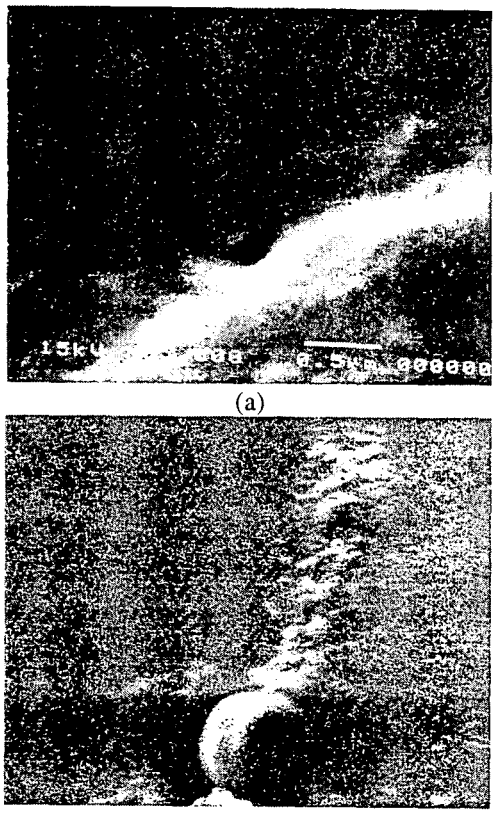

(a)

(b)

Figure 8 Images showing the presence of (a) a hole of diameter 0.3μm in the centre of a parabolic marking, at magnifications of 750x ; (b) a particle of at 15000x

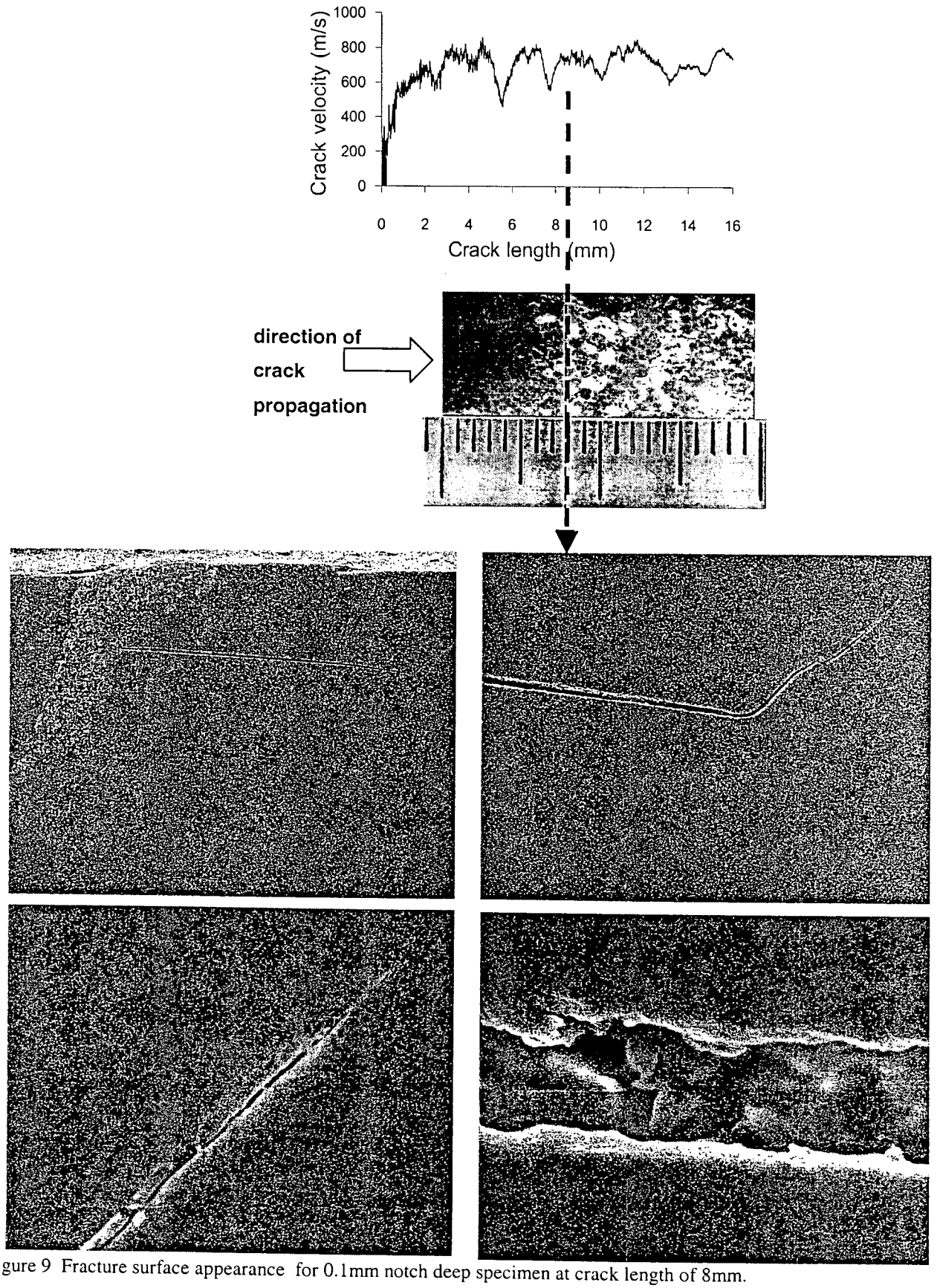

Figure 9 Fracture surface appearance for 0.1mm notch deep specimen at crack length of 8mm.

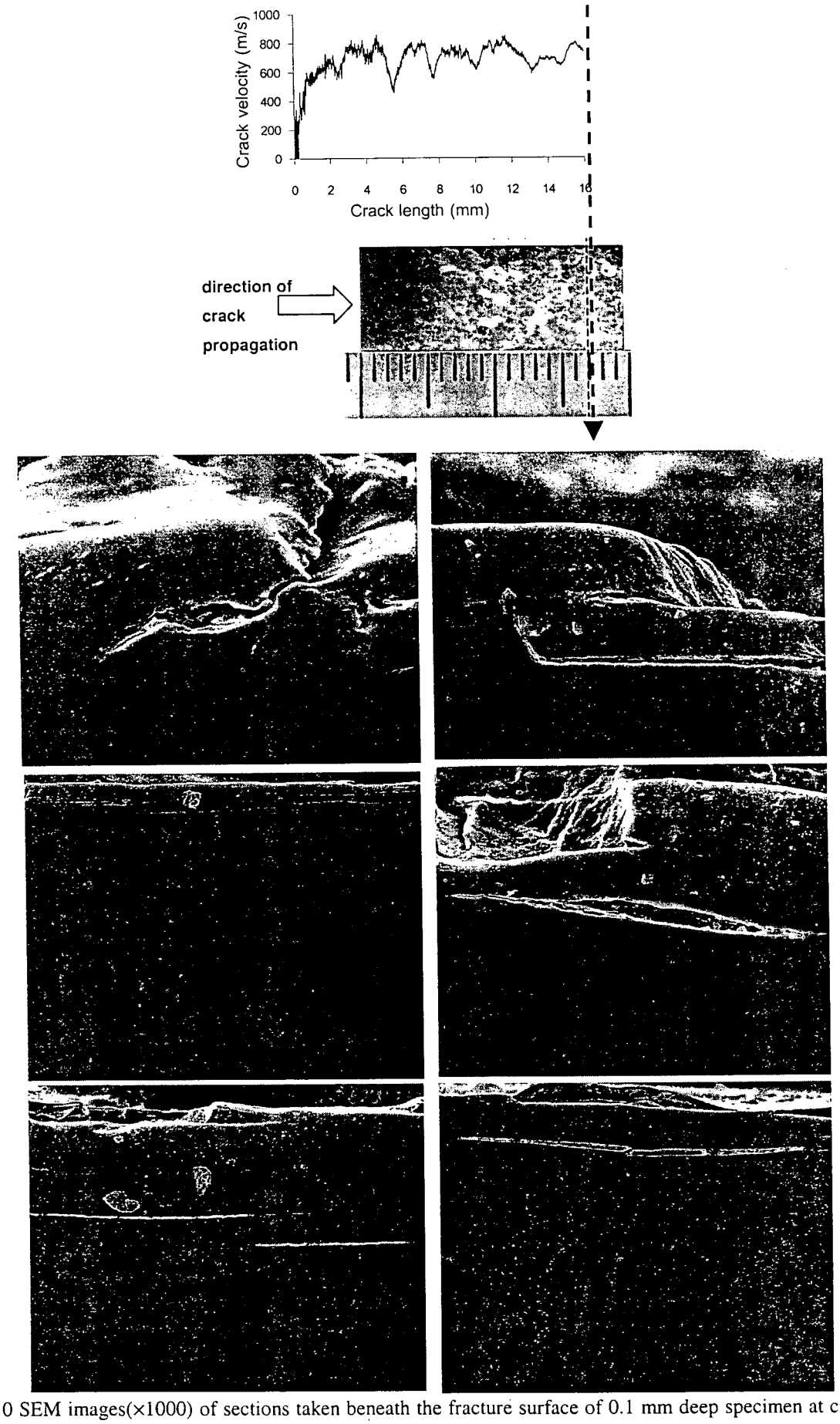

Figure 10 SEM images(×1000) of sections taken beneath the fracture surface of 0.1 mm deep specimen at crack length of 17mm